Acta Cryst. (1999). B**55**, 35–44

Disorder determined by high-resolution powder diffraction: structure of pentamethylcyclopentadienyllithium

Robert E. Dinnebier,[a]* Martin Schneider,[a] Sander van Smaalen,[a] Falk Olbrich[b] and Ulrich Behrens[c]

[a]*Lehrstuhl für Kristallographie, Universität Bayreuth, D-95440 Bayreuth, Germany,* [b]*Chemisches Institut, Otto-von-Guericke-Universität Magdeburg, D-39106 Magdeburg, Germany, and* [c]*Institut für Anorganische und Angewandte Chemie, Universität Hamburg, Martin-Luther-King-Platz 6, D-20146 Hamburg, Germany.*
E-mail: robert.dinnebier@uni-bayreuth.de

(*Received 27 February 1998; accepted 15 May 1998*)

Abstract

The crystal structure of pentamethylcyclopentadienyllithium, $[Li(C_{10}H_{15})]$ (LiCp*), has been determined from a high-resolution powder pattern by modelling and the maximum entropy method (MEM). The compound crystallizes in space group $R3m$ with lattice parameters $a = b = 14.7711\,(5)$, $c = 3.82206\,(6)$ Å and $V = 722.19\,(4)$ Å^3 ($Z = 3$). LiCp* forms polymeric 'multidecker' chains along the c axis. The pentamethylcyclopentadienyl anions are coplanar with each other and show threefold rotational disorder. The MEM calculations did not only confirm the structural model and the type of disorder, but also discovered additional symmetry compared with the Rietveld analysis. This is the first solid-state structure of a Lewis-base-free alkali metal Cp* compound.

1. Introduction

Base-free organolithium compounds have drawn special interest for many years because of their widespread use in organometallic chemistry and their suitability for theoretical studies and *ab initio* calculations (Weiss, 1993; Setzer & Schleyer, 1985). Among them are cyclopentadienyllithium (LiCp) and pentamethylcyclopentadienyllithium (LiCp*), which are among the most important reactants in synthetic organometallic chemistry. Over the last 25 years LiCp* has been used extensively as a precursor for the preparation of complexes of transition metals, rare earth metals and main group metals with Cp* (Ahlrichs *et al.*, 1996; Fokken *et al.*, 1996; Müller *et al.*, 1996). Despite its widespread use in synthesis, crystallographic studies of LiCp* or Lewis-base adducts of LiCp* have not been published to date (Allen *et al.*, 1991), although the structures of Lewis-base adducts are well known for related organolithium compounds, *e.g.* LiC_5H_4Me-(tmeda) (Hammel *et al.*, 1990), $LiC_5H_2(SiMe_3)_3$(thf) (Jutzi *et al.*, 1989) and $LiC_5(SiHMe_2)_5$(Ph-CO-Ph) (Sekiguchi *et al.*, 1993).

Single crystals of sufficient size for X-ray diffraction experiments have not been prepared so far, presumably because LiCp* is either insoluble or, when dissolved, complex compounds containing solvent molecules crystallize out. It should be noted that this problem hinders the structure solution of most base-free organolithium compounds (Weiss, 1993). Here we present the crystal structure of LiCp* as determined by means of high-resolution powder diffraction. The same approach has been previously applied successfully to determine the crystal structures of methyllithium, cyclopentadienyllithium and phenyllithium (Weiss *et al.*, 1990; Dinnebier *et al.*, 1997, 1998).

Accurate structure determinations of compounds with unsubstituted cyclopentadienyl and its permethylated counterpart are further complicated by the presence of disorder. Low barriers exist for rotation about an axis perpendicular to the molecular plane of the fivefold symmetric Cp and Cp* rings, with activation energies in the range 2–12 kJ mol^{-1} (Braga, 1992). Rotational disorder pertaining to Cp has been found for many molecular MCp_2 compounds, such as $FeCp_2$ and $CaCp_2$ (Willis, 1961; Zerger & Stucky, 1974). In the crystalline state disorder may persist and then lead to a higher symmetry of the structure than would have been possible without disorder. Here we will present evidence that Cp* has threefold rotational disorder in crystals of LiCp*, related to the symmetry axes in the space group $R3m$.

For many types of disorder it is difficult to devise an appropriate model based on atoms and harmonic displacement parameters. It can be necessary to use many different sites, each one with a partial occupancy by the atoms. A model which leads to a good fit to the data often requires the introduction of anharmonic displacement parameters (Kuhs, 1992). In either case, many additional parameters are introduced beyond those necessary for an ordered structure model and high correlations between these parameters are often observed. Except for simple cases, these features make it impossible to refine disordered structures against powder diffraction data because of the strongly reduced information compared with single-crystal diffraction. Alternatively, information on disorder can be obtained from a Fourier map generated from the phases of the structure factors calculated for the 'best' model and

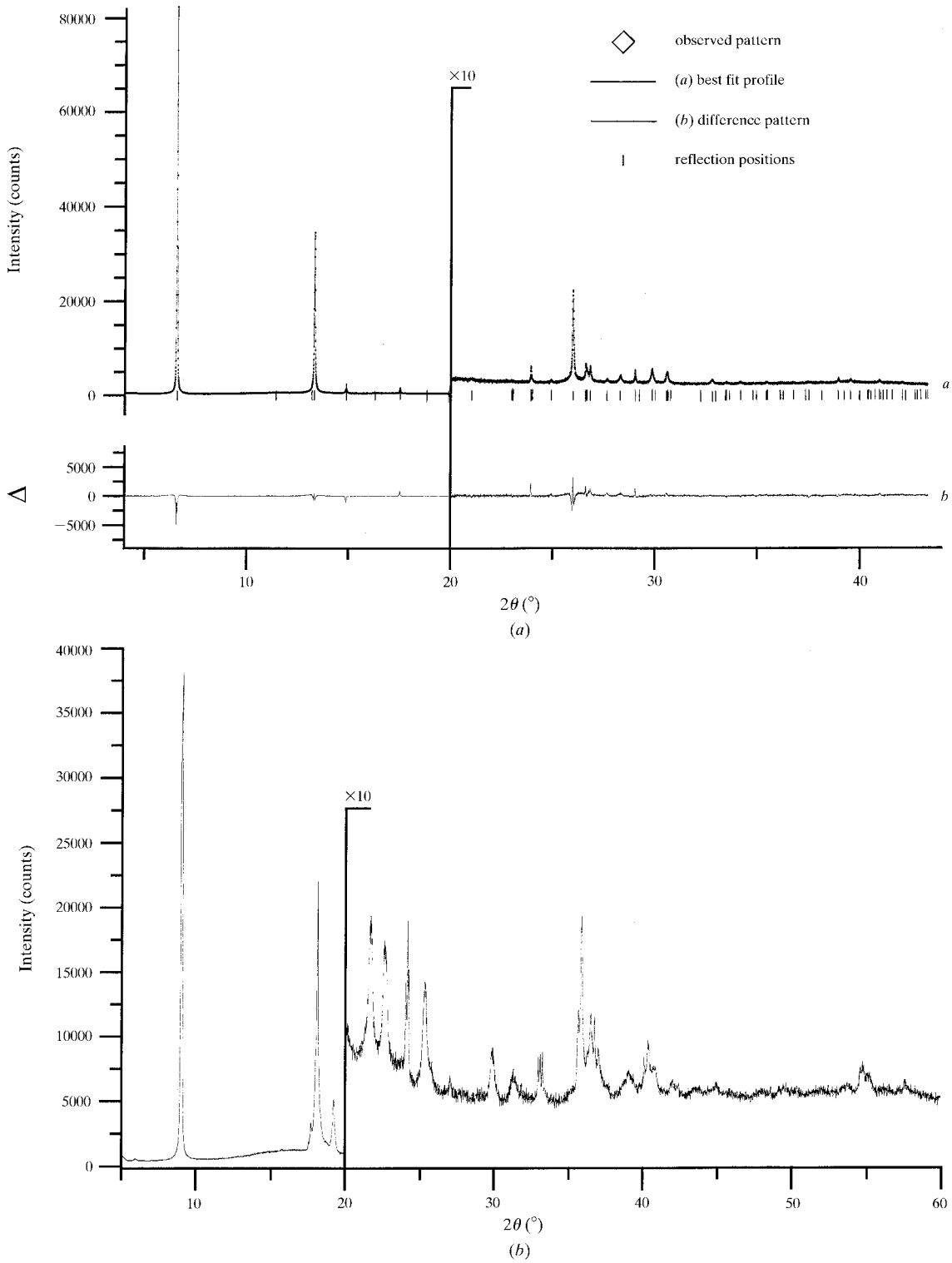

Fig. 1. (*a*) Scattered intensity of the room-temperature phase of pentamethylcyclopentadienyllithium (LiCp*) as a function of diffraction angle 2θ. Shown are the observed pattern (diamonds), the best Rietveld fit profile in $R3$ (line *a*), the difference curve between observed and calculated profiles (line *b*), and the reflection markers (vertical bars). The wavelength λ was 0.84979 (1) Å. The higher-angle part starting at $2\theta = 20^\circ$ is enlarged by a factor of 10 for clarity. The R values are $R_p = 0.0561$, $R_{wp} = 0.0832$, $R_{Bragg} = 0.1660$. (*b*) Scattered intensity of the low-temperature phase of pentamethylcyclopentadienyllithium (LiCp*) at 25 K as a function of diffraction angle. The wavelength λ was 1.15031 (1) Å. The higher-angle part starting at $2\theta = 20^\circ$ is enlarged by a factor of 10 for clarity.

their observed intensities. Again, powder diffraction cannot lead to reliable results, because the intensities are not known for many of the reflections. Here we will use the maximum entropy method (MEM) to study the disorder in LiCp*.

The MEM is gaining popularity in many branches of science and engineering. In crystallography the MEM has been used to determine the electron density from diffraction data independent of a structure model (Gilmore, 1996). Therefore, it is particularly suited to determining the structural aspects of disorder and anharmonic vibrations (Papoular *et al.*, 1991; Bagautdinov *et al.*, 1998). Usually the MEM requires the phases of the Bragg reflections, as obtained from refinement. In cases where the individual intensities can be determined for a sufficient number of reflections the MEM can also be applied to powder diffraction data. A special procedure for powder diffraction data allows the use of the information contained both in resolved and in overlapping reflections (Sakata & Sato, 1990). In the present study the MEM is used to determine the electron density due to disorder and anharmonic motion in crystals of LiCp*. Evidence is presented that Cp* occurs in three equivalent orientations related to threefold rotations about an axis perpendicular to the molecular planes. Differences and similarities between the MEM and the results from Rietveld refinements are discussed.

2. Experimental

LiCp* was prepared by a method similar to that of Kohl *et al.* (1986). Pentamethyl-1,3-cyclopentadiene was dissolved in tetrahydrofuran and *n*-butyllithium was added to give a white precipitate after stirring for 5 h at 328 K. The solid was separated from the liquid, washed with diethyl ether and dried in a vacuum at 0.01 Torr (1 Torr = 133.322 Pa). A yield of 85% was obtained, corresponding to 1.48 g of a white air- and moisture-sensitive powder.

For the X-ray diffraction experiments the sample was loaded into a glass capillary (Hilgenberg, glass No. 50, 0.7 mm diameter) and sealed. A high-resolution X-ray powder pattern was recorded in transmission mode at beamline BM16 at the European Synchrotron Radiation Facility (ESRF) (Fitch, 1997). X-rays of wavelength 0.84979 (1) Å were selected by a double Si(311) sagitally focusing monochromator. The diffracted beam was analysed with a nine-crystal analyser stage [nine Ge(111) crystals with an angular separation of $\sim 2^\circ$] and detected with nine Na(Tl)I scintillation counters simultaneously. The intensity of the incoming beam was monitored by an ionization chamber and these values were used to normalize the diffracted intensities. Data were collected at room temperature in continuous scanning mode. For analysis, the data from the different detectors were combined and converted to step-scan data. Although θ scans did not show serious crystallite size effects, the sample was rotated around θ during measurement to improve particle statistics. Low-angle diffraction peaks had an FWHM (full-width at half maximum) of $2\theta = 0.061^\circ$, significantly broader than the resolution of the spectrometer, which is estimated to be as good as $2\theta = 0.002^\circ$.†

Table 1. *Crystallographic data for the room-temperature structure of LiCp**

Formula	$[Li(C_{10}H_{15})]$
Formula weight (g mol^{-1})	142.171
Space group	*R*3*m*
$a = b$ (Å)	14.7711 (5)
c (Å)	3.82206 (6)
V (Å^3)	722.19 (4)
Z	3
D_{calc} (g cm^{-3})	0.980
2θ range (°)	0–68.03
Step size (2θ, °)	0.005
Counting time (h)	7
Wavelength (Å)	0.84979 (1)

Data reduction was performed using the program *GUFI* (Dinnebier, 1993). Indexing with *ITO* (Visser, 1969) led to a body-centred monoclinic cell which could be transformed to a rhombohedral cell. Lattice parameters for the hexagonal setting are $a = b = 14.7711$ (5), $c = 3.82206$ (6) Å and $V = 722.19$ (4) Å^3 with $Z = 3$. The observed extinction rules were only compatible with the space groups $R3$, $R\bar{3}$, $R32$, $R3m$ and $R\bar{3}m$. All these space groups have much higher symmetry than allowed by the molecular symmetry, thus providing strong evidence for disorder (Fig. 1*a*, Table 1).

To obtain reliable intensities a LeBail-type fit was performed using the program *GSAS* (LeBail *et al.*, 1988; Larson & Von Dreele, 1990). The peak profile function was modelled using a multi-term Simpson's rule integration of the pseudo-Voigt function (Thompson *et al.*, 1987). The asymmetry in the low-angle region was modelled according to Finger *et al.* (1994) leading to a strongly improved fit and therefore better profile R factors. A description of the background as obtained from a manual fit was used for all refinements. Peaks along (h00, 0k0) showed some anisotropy in the FWHM, which could not be satisfactorily modelled using the uniaxial strain option in *GSAS*. Together with the lattice parameters and the zero shift, a total of 11 parameters were refined in the LeBail fit, producing a set of 24 intensities of individual reflections and 60 intensities of groups of overlapping reflections. They were used in the MEM calculations and to define the Bragg R value of the Rietveld refinement (Fig. 1*a*).

Low-temperature scans were performed at the high-resolution powder beamline X3B1 of the National Synchrotron Light Source at Brookhaven National Laboratory. LiCp* was cooled down to 25 K in a closed-cycle helium cryostat. A phase transition was observed

† Supplementary data for this paper are available from the IUCr electronic archives (Reference: SE0236). Services for accessing these data are described at the back of the journal.

at ~240 K, indicated by the onset of a broadening of the diffraction maxima. This phase transition was found to be reversible because the diffraction maxima sharpen again on heating the sample to room temperature. A complete scan was taken at 25 K using a wavelength of 1.15031 (1) Å for 6.2 s at each 2θ in steps of 0.01° from 5 to 35.0° and for 12.2 s at each 2θ from 35 to 65.0° (Fig. 1*b*). The pattern of the low-temperature phase could not be indexed unambiguously. In addition, LeBail fits of several superstructures with monoclinic and orthorhombic symmetries based on the orthohexagonal cell have been tried. None gave a satisfactory fit. This failure is attributed to extreme line broadening with many closely overlapping reflections. It is very likely that there is at least partial order of the Cp* molecules at low temperatures, which often results in very low symmetry as in the case of triclinic $FeCp_2$ below 148 K (Calvarin & Berar, 1975).

3. Refinement and MEM calculations

Solution of the structure of the room-temperature phase was tried by direct methods using the program *SIRPOW* (Cascarano *et al.*, 1992). All attempts using different sets of starting parameters failed. This can be understood in view of the heavy peak overlap and the reduction of local electron density due to strong disorder.

Owing to the similarity between the length of the chain axis of the structure of LiCp (Dinnebier *et al.*, 1997) and the short axis of LiCp* it was supposed that a strong structural relationship exists between these two compounds. This could also be expected for chemical reasons. Consequently, a starting model was developed for the structure of LiCp* based on infinite multidecker chains of alternating Li atoms and disordered Cp* rings. For the Rietveld refinement all profile and lattice parameters were fixed at the values obtained by the LeBail fit and only the structural parameters were allowed to vary (Rietveld, 1969). Structure determinations of other Cp* compounds have shown that the Cp^{*-} anion can be regarded as rigid (Williams *et al.*, 1990). The carbon–carbon distances of the regular inner ring are 1.41 (3) Å and the carbon–carbon distances between the inner and outer rings are 1.51 (3) Å. Deviations from planarity are usually less than 0.005 Å. Under the assumption that the shape of the molecule remains close to its ideal form, the number of degrees of freedom could be reduced dramatically by the introduction of a rigid body for the Cp* ring. This reduced the number of refinable positional parameters of non-H atoms from 30 to 6 (3 rotational and 3 translational parameters). Due to symmetry restrictions in *R*3, the only remaining parameter was the rotation φ around the crystallographic *c* axis (chain axis). The effect was a strong increase in the ratio between linearly independent observations and parameters, and a considerable stabilization of the refinement process. *GSAS* (Larson & Von Dreele, 1990) allows the additional refinement of the bond lengths of two different carbon–carbon distances, while keeping the fivefold symmetry as the only constraint for the Cp* molecule. The carbon–carbon distances refined beyond reasonable values, indicating a high correlation between these parameters. The best fit obtained by the Rietveld method was not entirely satisfactory (Fig. 1*a*). The angle φ converged to a value which was only 2° (standard uncertainty 3°) different from a structure with additional mirror symmetry, indicating a possible higher symmetry of *R*3*m*. Subsequent Rietveld refinements in *R*3*m* led to the same $R_{\rm Bragg}$ value as in *R*3, but to a profile *R* value $R_p = 0.0715$ compared with $R_p = 0.0562$ for *R*3 symmetry, indicating a significantly better fit in *R*3 than in *R*3*m*. Using the Rietveld method it was not possible to determine the symmetry and the type of disorder unambiguously.

Therefore, we decided to study the electron density by the MEM. The *MEED* program package was used (Kumazawa *et al.*, 1993). All calculations were carried out on a Silicon Graphics Octane with two 175 MHz R10000 processors and 384 Mbyte of RAM. The required time for the calculations was between 0.5 and 40 h, depending on space-group symmetry, the value of the Lagrange multiplier and the criterion of convergence.

The MEM searches for the electron density corresponding to the maximum value of the entropy, subject to conditions provided by the experiment. The electron density is described in discrete form, leading to an entropy defined as

$$S = -\sum_{j=1}^{N} \rho_j \log(\rho_j/\omega_j), \tag{1}$$

where N is the number of pixels in the unit cell, ρ_j is the electron density in pixel j and ω_j is the initial value of the electron density or prior (Gilmore, 1996). Here, we used a division of the unit cell into 72 × 72 × 32 pixels, corresponding to a resolution of 0.21 × 0.21 × 0.12 Å along the cell axes.

The *MEED* program uses a single constraint, incorporated into the optimization process by a single Lagrange undetermined multiplier λ (Sakata & Sato, 1990; Kumazawa *et al.*, 1993). A value of $\lambda = 0.0001$ was found suitable for all calculations reported here. The constraint of the form $C = 0$ has two types of contributions. The first was termed an *F*-type constraint, which originates from the reflections with known phases according to

$$\chi_F^2 - N_1 = \left[\sum_{i=1}^{N_1} |F_{\rm MEM}(\mathbf{H}_i) - F_{\rm obs}(\mathbf{H}_i)|^2/\sigma^2(\mathbf{H}_i)\right] - N_1 = 0, \tag{2}$$

where N_1 is the number of observed reflections with known phases, $F_{\rm obs}(\mathbf{H})$ is the observed structure factor

including its phase information and $\sigma(\mathbf{H})$ is its standard uncertainty, and $F_{\mathrm{MEM}}(\mathbf{H})$ is the calculated structure factor obtained by discrete Fourier transformation of the electron density ρ_{MEM}. The G constraint incorporates the information contained in scattering maxima due to overlapping reflections. It is defined as

$$\chi^2_G - N_2 = \left[\sum_{j=1}^{N_2} |G^j_{\mathrm{MEM}} - G^j_{\mathrm{obs}}|^2/\sigma_j^2\right] - N_2 = 0 \quad (3)$$

with

$$G^j_{\mathrm{MEM}} = \left\{\sum_{i=1}^{n_j}[m_i|F_{\mathrm{MEM}}(\mathbf{H}_i)|^2]/\sum_{i=1}^{n_j} m_i\right\}^{1/2}, \quad (4)$$

where G^j_{obs} is the square root of the observed intensity of the scattering maximum at $|\mathbf{H}_j|$, n_j is the number of reflections contributing to the group j and m_i is the multiplicity of the ith contributing reflection, N_2 is the number of groups of overlapping reflections, and σ_j is the standard uncertainty of G^j_{obs}.

The first *MEED* calculation was based on constraints using $F_{\mathrm{calc}}(\mathbf{H})$ from the best Rietveld fit in $R3$ as $F_{\mathrm{obs}}(\mathbf{H})$. Since phases are known for all reflections, only the F-type constraint was required and $N_1 = 157$ and $N_2 = 0$ were used. Using a constant density as prior (ω_j = 0.3240 e Å^{-3}), convergence was reached at $R = 0.0291$. The resulting electron density $\rho^{\mathrm{calc}}_{\mathrm{MEM}}$ clearly shows 15 maxima on an outer circle, whereas the expected 15 maxima on the inner circle have coalesced into a ring of constant density (Fig. 2). Further analysis of $\rho^{\mathrm{calc}}_{\mathrm{MEM}}$ shows that this MEM calculation did reproduce exactly the model used to generate $F_{\mathrm{calc}}(\mathbf{H})$. Firstly, this result shows that the MEM and the parameters chosen are suitable for the study of the present system. Secondly, the MEM is found to be superior over a Fourier map calculated with the same reflections (Fig. 3).

The second *MEED* calculation used observed intensities [$F_{\mathrm{obs}}(\mathbf{H})$ and G^j_{obs}] from the LeBail fit, together with phases from the Rietveld fit in $R3$. Both types of constraints were necessary ($N_1 = 24$, $N_2 = 60$). The observed intensities were scaled towards the standard scattering power of one unit cell. Using a flat prior, convergence was reached at $R = 0.0251$. Despite a low R factor, which is similar to those of other $\rho^{\mathrm{calc}}_{\mathrm{MEM}}$'s, the resulting electron density did show many artifacts (Fig. 4).

The third *MEED* calculation was based on the same constraints as the second, but a different prior was used. The result of the first *MEED* calculation $\rho^{\mathrm{calc}}_{\mathrm{MEM}}$ was taken as the initial electron density [$\omega_j = (\rho^{\mathrm{calc}}_{\mathrm{MEM}})_j$]. Convergence was now reached after 120 000 cycles at R = 0.0213, resulting in an electron density ρ^{R3}_{MEM}. Note that the agreement between F_{MEM} based on $\rho^{\mathrm{calc}}_{\mathrm{MEM}}$ and the F plus G constraint based on the LeBail intensities was only $R = 0.3513$. This shows the large gap between the model (to which $\rho^{\mathrm{calc}}_{\mathrm{MEM}}$ is equivalent) and the measured scattering data. Nevertheless, $\rho^{\mathrm{calc}}_{\mathrm{MEM}}$ and ρ^{R3}_{MEM} have similar appearance and both show the threefold disordered Cp* molecule (Fig. 5). Differences are also present, of which one pertains to the symmetry of the electron density. $\rho^{\mathrm{calc}}_{\mathrm{MEM}}$ exhibits a molecular mirror plane which deviates by 2° from a possible crystallographic mirror (Fig. 2), in complete accordance with the Rietveld model. ρ^{R3}_{MEM}, however, is deformed such that the maxima are closer to positions corresponding to a crystallographic mirror symmetry than those of $\rho^{\mathrm{calc}}_{\mathrm{MEM}}$ (Fig. 5). To accommodate the reflection phases of $R3$, the values of the maxima now violate the mirror symmetry. It was therefore concluded that the experiment did not contain evidence for a deviation from $R3m$ symmetry. Convergence of a calculation with the MEM in $R3m$ was equally good as in $R3$ with $R = 0.0214$, resulting in $\rho^{R3m}_{\mathrm{MEM}}$ (Fig. 6*a*).

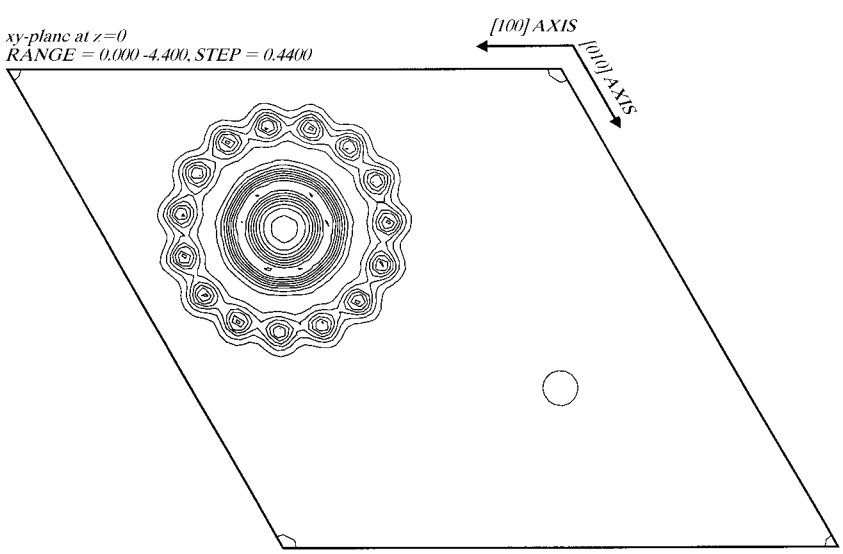

Fig. 2. Electron density map of LiCp* in the plane $z = 0$ obtained after a MEM calculation using the calculated structure factors of the best Rietveld fit in $R3$ as experimental data (157 F and 0 G constraints, R = 0.0318). The threefold disorder of the Cp* molecule is clearly visible. Note the 2° deviation between the molecular mirror symmetry and $R3m$ symmetry.

The final result of the calculation using the MEM in *R*3*m* does show the molecular nature of Cp* (Fig. 6*a*) as well as the Li atom at the expected position (Fig. 6*b*). A quantitative analysis of $\rho_{\rm MEM}^{R3}$ shows that the 15 maxima in the electron density, together with the ring-like maximum, closely match the atom positions of the Cp* molecule in three orientations (Fig. 7 and Table 2). The differences between $\rho_{\rm MEM}^{R3}$ and the model $\rho_{\rm MEM}^{\rm calc}$ lie in some fine details.

As is apparent from the comparison of Fig. 2 and Fig. 6(*a*), several of the 15 maxima in $\rho_{\rm MEM}^{R3}$ have a pear-like shape pointing outwards from the ring centre, contrary to the 15 maxima in $\rho_{\rm MEM}^{\rm calc}$, which are the superposition of partially overlapping spheres. We interpret this feature as well as the other differences between $\rho_{\rm MEM}^{R3}$ and $\rho_{\rm MEM}^{\rm calc}$ as being due to anharmonic contributions to the disorder of the Cp* molecule. The pear-like features then indicate that the molecules in different orientations also have different positions of their centres with respect to the point $(\frac{2}{3}, \frac{1}{3}, 0)$. Apart from rotations there is also a shift contribution to the disorder.

A final Rietveld refinement using *R*3*m* symmetry and rigid-body coordinates as found by MEM calculations did not give any improvement compared with previous refinements in *R*3*m* still having profile *R* factors worse by 2 absolute per cent compared with refinements in *R*3. It was neither possible to refine the C—C distance of the inner ring nor the C—C distance from the inner to the outer ring of the Cp* molecule individually. We attribute this to the high degree of disorder, the large number of overlapping reflections and the occurrence of anharmonic displacements which were not contained in the

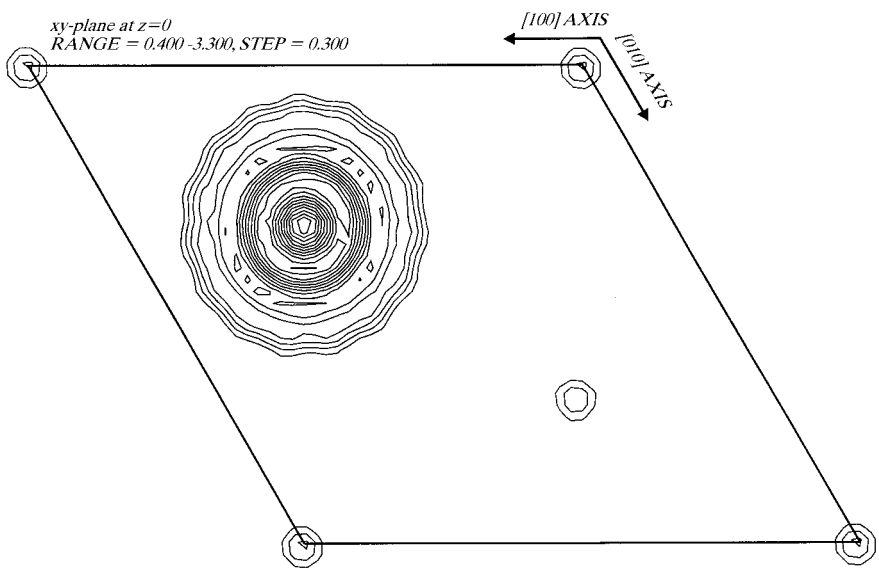

Fig. 3. Electron density map of LiCp* in the plane $z = 0$ obtained after Fourier analysis using the calculated structure factors of the best Rietveld fit in *R*3. The 15 maxima of the outer C atoms of the Cp* molecule are not visible. Although using the same set of data, the resolution is much lower compared with that of the MEM calculations (Fig. 2). This can be attributed to termination effects of the Fourier series.

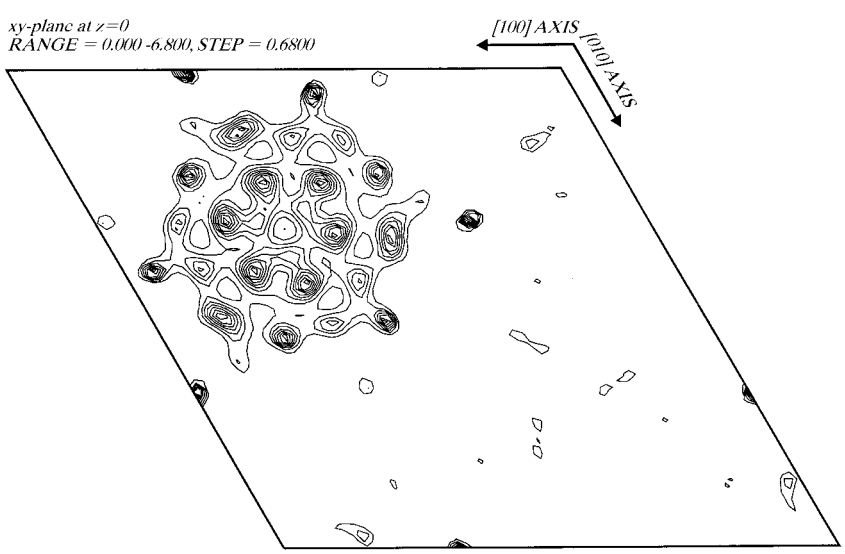

Fig. 4. Electron density map of LiCp* in the plane $z = 0$ obtained after a MEM calculation using the reflection intensities from the LeBail fit and the phases of non-overlapping reflections from a Rietveld fit in *R*3 (24 *F* and 60 *G* constraints, $R = 0.0251$). The MEM calculation started from a flat electron density. The threefold disorder of the Cp* molecule is barely visible. Note the occurrence of artifacts.

Table 2. *Positional parameters of LiCp* in R3m symmetry*

The standard uncertainty for the fractional coordinates derived by the MEM is estimated to be of the order 0.0007.

	x (MEM)	y (MEM)	z (MEM)	x (model)	y (model)	z (model)	U (model)	Fractional occupancy
Li	2/3	1/3	0.5	2/3	1/3	0.5	0.060	1
C11	—	—	0	0.714	0.427	0	0.062 (2)	1/3
C12	—	—	0	0.758	0.362	0	0.062 (2)	1/6
C13	—	—	0	0.677	0.258	0	0.062 (2)	1/6
C21	0.7810	0.5610	0	0.774	0.547	0	0.046 (3)	1/3
C22	0.8819	0.4055	0	0.876	0.400	0	0.046 (3)	1/6
C23	0.6929	0.1620	0	0.689	0.160	0	0.046 (3)	1/6

structure model, but which do not hamper the MEM in finding the optimal electron density. Attempts to model additional disorder by the **TLS** formalism failed.

4. Rotational barrier energy calculation

In order to understand the nature of the disorder, the rotational barrier of the Cp* ring was calculated. Lattice-energy calculations were performed by the method of atom–atom potentials. The program *CRYSCA* (Schmidt, 1995) was used with force-field parameters derived by Filippini & Gavezzotti (1993). It was assumed that the Li atom does not move away from its 3*m* position during a rotation of the Cp* fragment and that the rotational barrier is only determined by nonbonded interactions between Cp* fragments. Therefore, only interactions of van der Waals type between the atoms were included, with lithium treated as carbon and Cp* treated as a rigid body. The atomic positions of Li and the C atoms of the outer ring were taken directly from the MEM electron density map, whereas those for the C atoms of the inner rings have been calculated assuming a C—C distance between the rings of 1.54 Å. H-atom positions were calculated at a distance of 1.09 Å from the C atoms, according to the C_{5v} molecular symmetry of Cp* and tetrahedrally coordinated C atoms. All interactions up to 20 Å were included in the lattice sum. Charges were neglected, since their influence on the rotational barrier is less than 0.01 kJ mol^{-1}. With this potential the experimental lattice parameters a and b were reproduced with an accuracy of 0.001 Å, whereas bigger differences in c occurred. It should be noted that the length of the hexagonal c axis is mainly determined by Li—Cp* interactions and not by van der Waals forces. For the determination of the rotational barrier the lattice parameters were kept fixed and a series of structures was generated corresponding to different orientations of Cp*. To describe the crystal structure of LiCp* without disorder, the local crystal symmetry was set to *R*1. The Cp* molecules were rotated around the c axis in steps of 1°. The lowest energy was found for $\varphi = 0°$ (one C atom of each ring situated on a mirror plane in *R*3*m*), which corresponds to the orientation determined by MEM calculations. The rotational barrier was calculated to be 2.11 kJ mol^{-1}, which is small in comparison with other substituted or unsubstituted metallocenes in the solid state such as $FeCp_2^*$ (10–13.5 kJ mol^{-1}) or $FeCp_2$ (calculated 4.9–8.4 kJ mol^{-1}, experimental 4.6–9.6 kJ mol^{-1}, at room temperature; *e.g.* Carter & Murrell, 1980; Braga, 1992). Despite the larger size, the rotational barriers for Cp* and Cp are quite similar (Zanin *et al.*, 1992).

The energy barrier was found to be in good agreement with the periodic function

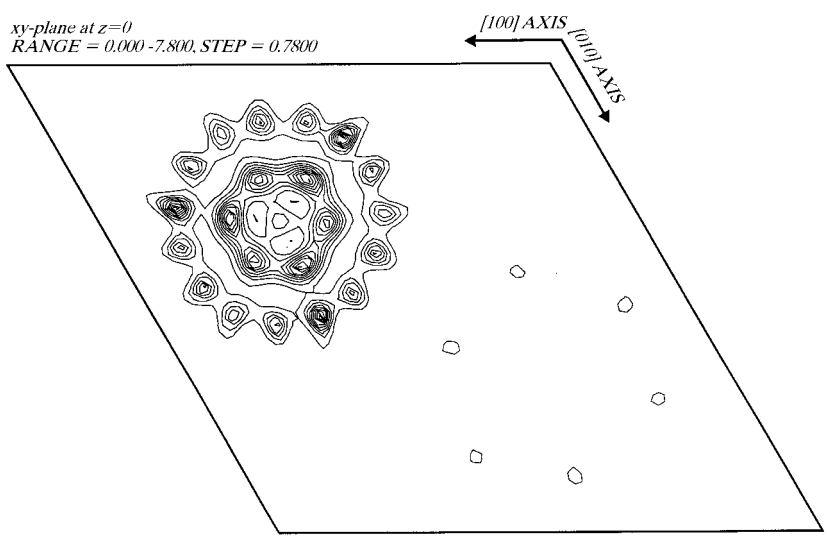

Fig. 5. Electron density map of LiCp* in the plane $z = 0$ obtained after a MEM calculation using the same constraints as in Fig. 4, but a prior defined by the electron density obtained from the MEM calculation using F_{calc} (Fig. 2). The Cp* molecule and the threefold disorder are clearly visible.

$$E(\varphi)\ (\mathrm{kJ\ mol^{-1}}) = (2.11/2)[1 - \cos(15\varphi)], \quad (5)$$

with φ being the rotational angle. This led to an angular probability of the orientation of the molecule of

$$\rho(\varphi) = 0.009 \exp\{0.43[1 - \cos(15\varphi)]\}. \quad (6)$$

The calculated energies and their fitting function as well as the calculated angular probability are shown in Fig. 8. It can be seen that the maximum of the calculated angular probability is consistent with the peaks from the electron density maps of the MEM calculation.

5. Discussion

The distances from the C atoms of the outer ring to the centre of the Cp* molecule as determined from ρ^{R3}_{MEM} lay between 2.75 (2) Å for C21 and 2.91 (2) Å for C23. Assuming a typical C(ring)—C(methyl) distance of 1.54 Å, this would lead to C—C(ring) distances between 1.42 and 1.61 Å. Whereas the lower limit is about the value expected for LiCp complexes (Evans *et al.*, 1992), any bond length beyond 1.45 Å has no chemical meaning. We attribute this to the occurrence of anharmonic displacements. The possible movements of a single molecule in the neighbourhood of six parallel disordered chains, which can be regarded as cylinders, are not uniform, leading to different bond lengths in different directions. The positions of the H atoms are not given. Except for very special cases, their positions cannot usually be determined experimentally by X-ray powder techniques, although their contribution to the profile is definitely measurable (Lightfoot *et al.*, 1993). Further-

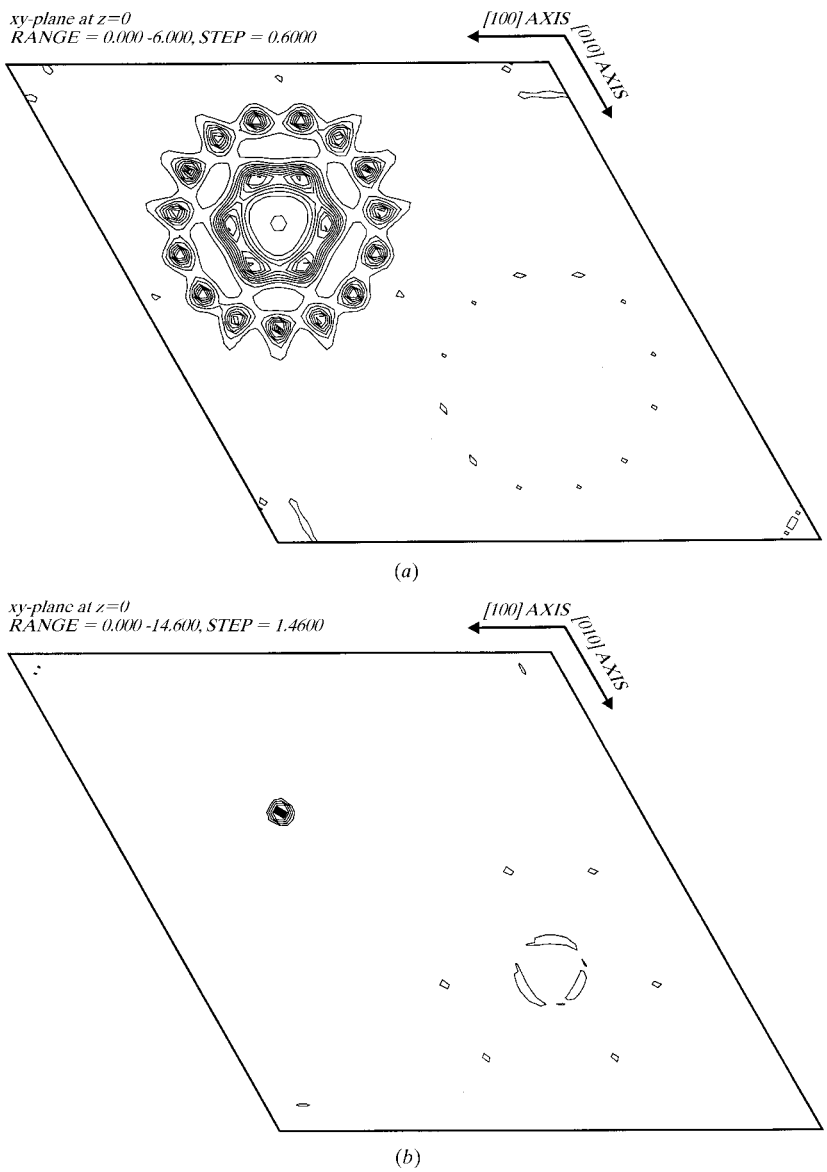

Fig. 6. (*a*) Electron density map of LiCp* in the plane $z = 0$ obtained after a MEM calculation using the reflection intensities from the LeBail fit and the phases of non-overlapping reflections from a Rietveld fit in *R*3*m* (24 *F* and 60 *G* constraints, $R = 0.0197$). The MEM calculation started from prior electron density calculated from calculated structure factors of a Rietveld fit in *R*3*m*. The threefold disorder of the Cp* molecule is clearly visible. (*b*) Electron density map of LiCp* in the plane $z = 0.5$ obtained after a MEM calculation as in Fig. 6(*a*), showing the position of the Li atom.

more, it can also be assumed that the H atoms of the methyl groups rotate freely at room temperature.

A perspective view of the chain structure of LiCp* without disorder is given in Fig. 9. LiCp* forms a similar type of 'multidecker' chain as its unsubstituted LiCp analogue (Dinnebier *et al.*, 1997) along the short *c* axis. The Li atoms are linearly coordinated by two η^5-bonded cyclopentadienyl rings. The Li—Cp*$_{cent}$ distance (where cent indicates centroid) could be determined with high precision as 1.911 (1) Å, since the repeat distance of the *c* axis is twice that of the Li—Cp*$_{cent}$ distance. This distance fits well in the range of distances from 1.79 (Jutzi *et al.*, 1985) to 2.09 Å (Malaba *et al.*, 1992) reported for other lithium cyclopentadienide complexes. It is slightly shorter than for unsubstituted LiCp [1.969 (1) Å; Dinnebier *et al.*, 1997], for $(C_5H_4SiMe_3)Li$ [1.957–1.982 Å; Evans *et al.*, 1992] and for $[LiCp_2]^-$ anions [1.969–2.008 Å; Harder & Prosenc, 1994; Wessel *et al.*, 1995]. All Cp* molecules in LiCp* are coplanar. The coordination of the Cp* rings to the Li atoms is symmetric, which means that a line between the centre of the Cp* rings and the Li atoms is not bent. In the case of LiCp this line is bent by 3.6°. In the structure of LiCp* as well as in LiCp, the chains are surrounded by six other chains. They differ in their relative shifts. In the LiCp structure a Cp ring is surrounded by four Li atoms and two Cp molecules, all in the molecular plane. Thus, two of the neighbouring chains are not shifted along **c**, whereas the other four are shifted by half their repeat length (1.968 Å). In LiCp* all six neighbouring chains are shifted alternately by either $+\frac{1}{3}$ or $-\frac{1}{3}$ ($\pm$1.274 Å) of their repeat distance. As a consequence, the Cp* ring is surrounded by six Li atoms which are out of the molecular plane by $\pm\frac{1}{6}$ ($\pm$ 0.637 Å) of the chain repeat unit. In contrast to LiCp, where the Cp rings are eclipsed, LiCp* shows threefold disorder of the Cp* molecules within the crystallographic *ab* plane. The disorder can be described by the average image of three superimposed Cp* rings having the same ring centre but different orientations regularly separated by 24°.

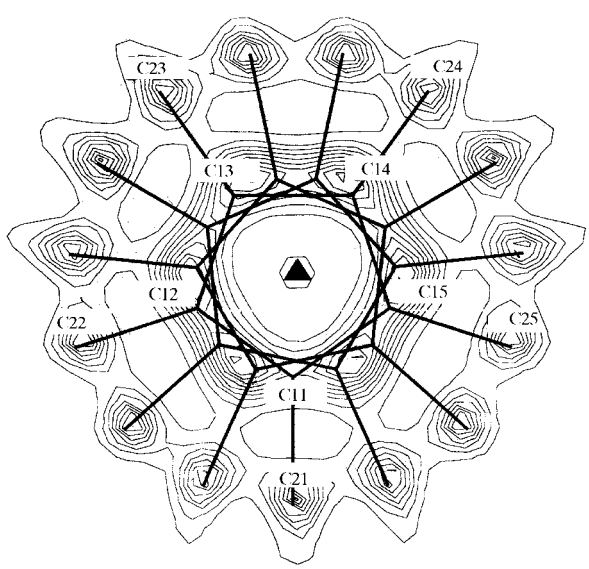

Fig. 7. Model for the disorder of the Cp* molecule in LiCp*. The electron density of the Cp* ring as obtained by MEM calculations (Fig. 6*a*) is plotted together with a molecular model. A triangle symbolizes the threefold axis. The atom labels for one Cp* ring are given (C11···C15 for the inner ring and C21···C25 for the outer ring). Note the negligible deviations from ideal symmetry for the outer C atoms.

6. Conclusions

Using the MEM it was possible to determine the type of disorder and to derive the existence of mirror planes in the crystal structure of LiCp* solely from powder data. It was found in the present case, with many overlapping reflections, that MEM calculations starting from a flat electron density will either diverge or converge to false minima. The use of a calculated electron density from the best available model as a prior was found to be necessary to reach the correct minimum. The importance of the prior has recently been shown by de Vries *et al.* (1996) for a different type of problem using single-crystal data. In all electron density maps derived by Fourier analysis the resulting electron densities were completely smeared out showing no detail of the disorder. We therefore conclude that the MEM method is superior to the Rietveld method in cases where disorder occurs.

We are grateful to Dr Martin Schmidt from Clariant GmbH for the calculations of the rotational energy barrier and to Dr Andy Fitch for his assistance during the measurement at the European Synchrotron Radia-

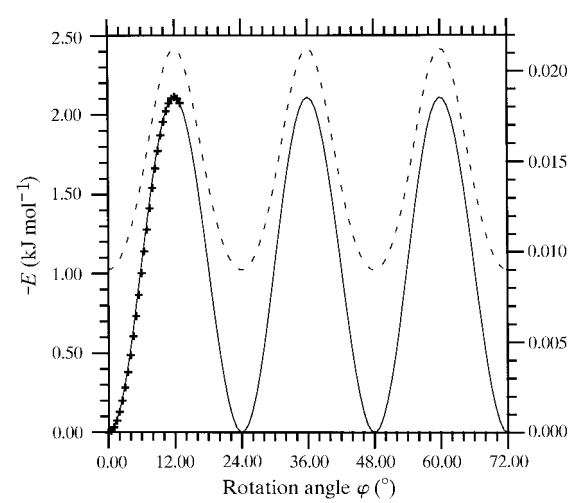

Fig. 8. Fitted rotational energy barrier (solid line), calculated rotational energy barrier from force-field calculations (plus signs) and angular probability (dashed line) of LiCp*.

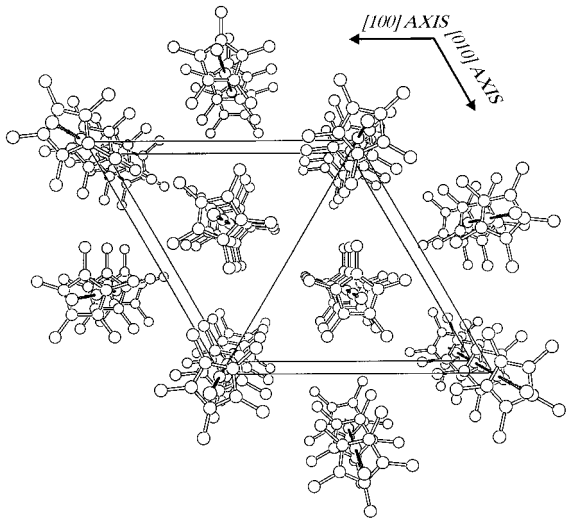

Fig. 9. Packing diagram of LiCp* without the threefold axis creating disorder ($P3_1$ rather than $R3m$ symmetry). A perspective view along the z axis with a view distance of 35 Å was chosen.

tion Facility (ESRF). Measurements at ESRF were carried out under the general user proposal CH-189. Research was carried out in part at the National Synchrotron Light Source (NSLS) at Brookhaven National Laboratory, which is supported by the US Department of Energy, Division of Materials Sciences and Division of Chemical Sciences. The SUNY X3 beamline at NSLS is supported by the Division of Basic Energy Sciences of the US Department of Energy under grant No. DE-FG02-86ER45231. Financial support by the Deutsche Forschungsgemeinschaft is gratefully acknowledged (Di 687/2-1, Sm 55/1, Be 760/10-1).

References

Ahlrichs, R., Fenske, D., Fromm, K., Krautscheid, H., Krautscheid, U. & Treutler, O. (1996). *Chem. Eur. J.* **2**, 238–244.
Allen, F. H., Davies, J. E., Galloy, J. J., Johnson, O., Kennard, O., Macrae, C. F., Mitchell, E. M., Mitchell, G. F., Smith, J. M. & Watson, D. G. (1991). *J. Chem. Inf. Comput. Sci.* **31**, 187–204.
Bagautdinov, B., Luedecke, J., Schneider, M. & van Smaalen, S. (1998). *Acta Cryst.* B**54**, 626–634.
Braga, D. (1992). *Chem. Rev.* **92**, 633–665.
Calvarin, G. & Berar, J. F. (1975). *J. Appl. Cryst.* **8**, 380.
Carter, S. & Murrell, J. N. (1980). *J. Organomet. Chem.* **192**, 399–408.
Cascarano, G., Favia, L. & Giacovazzo, C. (1992). *J. Appl. Cryst.* **25**, 310–317.
Dinnebier, R. E. (1993). Dissertation thesis, University of Heidelberg, Germany. (ISBN 3-89257-067-1.)
Dinnebier, R. E., Behrens U. & Olbrich, F. (1997). *Organometallics*, **16**, 3855–3858.
Dinnebier, R. E., Behrens, U. & Olbrich, F. (1998). *J. Am. Chem. Soc.* **120**, 1430–1433.
Evans, W. J., Boyle, T. J. & Ziller, J. W. (1992). *Organometallics*, **11**, 3903–3907.
Filippini, G. & Gavezzotti, A. (1993). *Acta Cryst.* B**49**, 868–880.
Finger, L. W., Cox, D. E. & Jephcoat, A. P. (1994). *J. Appl. Cryst.* **27**, 892–900.
Fitch, A. (1997). *BM16a*, http://www.esrf.fr/exp_facilities/BM16/handbook/handbook.html.
Fokken, S., Spaniol, T. P., Kang, H.-C., Massa, W. & Okuda, J. (1996). *Organometallics*, **15**, 5069–5072.
Gilmore, C. J. (1996). *Acta Cryst.* A**52**, 561–589.
Hammel, A., Schwartz, W. & Weidlein, J. (1990). *Acta Cryst.* C**46**, 2337–2339.
Harder, S. & Prosenc, M. H. (1994). *Angew. Chem. Int. Ed. Engl.* **33**, 1744–1746.
Jutzi, P., Leffers, W., Pohl, S. & Saak, W. (1989). *Chem. Ber.* **122**, 1449–1456.
Jutzi, P., Schlüter, E., Pohl, S. & Saak, W. (1985). *Chem. Ber.* **118**, 1959–1967.
Kohl, F. X., Kanne, D. & Jutzi, P. (1986). *Organomet. Synth.* **3**, 381–383.
Kuhs, W. F. (1992). *Acta Cryst.* A**48**, 80–98.
Kumazawa, S., Kubota, Y., Takata, M., Sakata, M. & Ishibashi, Y. (1993). *J. Appl. Cryst.* **26**, 453–457.
Larson, A. C. & Von Dreele, R. B. (1990). Report LAUR 86-748. Los Alamos National Laboratory, Los Alamos, USA.
LeBail, A., Duroy, H. & Fourquet, J. L. (1988). *Mater. Res. Bull.* **23**, 447–452.
Lightfoot, P., Metha, M. A. & Bruce, P. G. (1993). *Science*, **262**, 883–885.
Malaba, D., Chen, L., Tessier, C. A. & Youngs, W. J. (1992). *Organometallics*, **11**, 1007–1009.
Müller, C., Bartsch, R., Fischer, A., Jones, P. G. & Schmutzler, R. (1996). *J. Organomet. Chem.* **512**, 141–148.
Papoular, R. J., Prandl, W. & Schiebel, P. (1991). *Maximum Entropy and Bayesian Methods*, edited by C. R. Smith *et al.* Dordrecht: Kluwer Academic Publishers.
Rietveld, H. M. (1969). *J. Appl. Cryst.* **2**, 65–71.
Sakata, M. & Sato, M. (1990). *Acta Cryst.* A**46**, 263–270.
Schmidt, M. U. (1995). *Kristallstrukturberechnungen metallorganischer Verbindungen*. Dissertation (in German). Aachen: Verlag Shaker.
Sekiguchi, A., Sugai, Y., Ebata, K., Kabuto, C. & Sakurai, H. (1993). *J. Am. Chem. Soc.* **115**, 1144–1146.
Setzer, W. N. & Schleyer, P. (1985). *Adv. Organomet. Chem.* **24**, 353–451.
Thompson, P., Cox, D. E. & Hastings, J. B. (1987). *J. Appl. Cryst.* **20**, 79–83.
Visser, J. W. (1969). *J. Appl. Cryst.* **2**, 89–95.
Vries, R. Y. de, Briels, W. J. & Feil, D. (1996). *Phys. Rev. Lett.* **77**, 1719–1722.
Weiss, E. (1993). *Angew. Chem. Int. Ed. Engl.* **32**, 1501–1523.
Weiss, E., Lambertsen, T., Schubert, B., Cockcroft, J. K. & Wiedenmann, A. (1990). *Chem. Ber.* **123**, 79–81.
Wessel, J., Lork, E. & Mews, R. (1995). *Angew. Chem. Int. Ed. Engl.* **34**, 2376–2378.
Williams, R. A., Hanusa, T. P. & Huffmann, J. C. (1990). *Organometallics*, **9**, 1128–1134.
Willis, B. T. M. (1961). *Acta Cryst.* **13**, 1088.
Zanin, I. E., Antipin, M. Yu., Struchkov, Yu. T., Kudinov, A. K. & Rybinskaya, M. I. (1992). *Metallorg. Chim.* **5**, 579–589. (In Russian.)
Zerger, R. & Stucky, G. (1974). *J. Organomet. Chem.* **80**, 7–17.